



OPEN Dementia classification using two-channel electroencephalography features

Kuk-In Jang¹, Yeong In Kim², Hyo Jin Ju³, Sang Joon An^{2,4,6}✉ & Pyong Woon Park^{1,5,6}✉

This study aimed to develop a novel classification model using wearable two-channel electroencephalography (EEG) data to differentiate between patients with dementia and normal controls (NCs). We employed an extreme gradient boosting (Xgboost) model combined with recursive feature elimination with cross-validation (RFECV) to classify patients and NCs. The study included 54 NCs and 29 patients with dementia. Resting-state EEG was recorded, and Mini-Mental Status Exam (MMSE) and Clinical Dementia Rating (CDR) assessments were conducted. Significant differences were observed in peak frequency (PF), alpha (A), theta (T), the ratio of alpha to theta (A/T), the ratio of alpha to low-beta (A/BL), and coherence (CH) between patients and NCs. Patients with dementia exhibited decreases in PF, CH_A/T, CH_A/BL, A/T, and A/BL, while an increase in T was noted. The primary finding was that the Xgboost model, a tree ensemble classification, achieved a balanced accuracy of 97.05% with the RFECV-selected feature, which was PF. This study suggests that the novel Xgboost with RFECV classification model using two-channel EEG data could be a valuable tool for diagnosing dementia.

Keywords Two-channel EEG, Dementia, Xgboost, Classification, Machine learning

Dementia is a brain disease characterized by declines in memory, cognition, social abilities, and communication skills. It affects 5–10% of people aged 65 and older¹. In South Korea, the prevalence of dementia has been reported to be between 8.2% and 10.4%². This condition significantly impacts the quality of life for those affected³. Early diagnosis and intervention are crucial in managing the disease⁴.

Several diagnostic modalities have been suggested for dementia^{5–7}. The importance of having precise and convenient diagnostic methods is highlighted by the need for immediate and clinically compatible assessments. Measuring neural activity and cognitive function are crucial for diagnosing dementia. Conventional diagnostic approaches include examinations of neurocognitive tasks, blood tests, genetic analyses, and neuroimaging techniques such as magnetic resonance imaging (MRI) and positron emission tomography (PET)^{8,9}. These tools, however, are expensive and involve complex procedures to assess pathophysiology.

To meet the requirement for simplified and accurate assessments, electroencephalography (EEG) is a recommended non-invasive technique for diagnosing dementia^{10,11}. Changes in various EEG frequencies have been reported as biomarkers in patients with dementia¹². Compared to healthy individuals, patients with dementia exhibit a global increase in theta activity, which correlates with neuropsychological measures and the total amount of tau¹³. Conversely, a decrease in alpha power is a potential biomarker of dementia and is associated with a smaller nucleus basalis volume, which modulates cortical activity and higher-order cognitive functions¹⁴. Patients with Lewy body dementia show a lower peak frequency compared to those with Alzheimer's disease (AD)¹⁵. Beta activity could also indicate visual cognitive performance, as its reduction is observed in senior subjects¹⁶. However, using multi-channel EEG involves uncomfortable procedures and is time-consuming to set up for recording. Previous studies have reported that wearable two-channel EEG device was effective in detecting neurophysiological abnormalities in patients with psychiatric disorders^{17,18}.

¹Corporate Research Institute, Panaxtos Corp, Seoul, Republic of Korea. ²Department of Neurology, International St. Mary's Hospital, Catholic Kwandong University College of Medicine, Incheon, Republic of Korea. ³The Convergence Institute of Healthcare and Medical Science, Catholic Kwandong University College of Medicine, Incheon, Republic of Korea. ⁴Department of Neurology, International St. Mary's Hospital, Catholic Kwandong University College of Medicine, Simgok-RO 100GIL 25, Seo-GU, Incheon Metropolitan City 22711, Republic of Korea. ⁵Corporate Research Institute, Panaxtos Corp., 3F Shindonga Tower, 33 Ogeum-ro 11-gil, Songpa-gu, Seoul 05543, Republic of Korea. ⁶These authors contributed equally: Sang Joon An and Pyong Woon Park. ✉email: neuroan@gmail.com; panipara@panaxtos.com

Tree model-based techniques, characterized by their hierarchical decision-making structure resembling a tree, have gained widespread adoption within clinical science^{19,20}. Among these techniques, extreme gradient boosting (Xgboost) stands out as a highly efficient and popular algorithm²¹. It enhances traditional gradient boosting with features like regularization to prevent overfitting, support for parallel and distributed computing to manage datasets, and advanced tree pruning techniques. Additionally, recursive feature elimination with cross-validation (RFECV) has emerged as a sophisticated method for feature selection^{22,23}. By iteratively removing less important features and integrating cross-validation, RFECV ensures robust feature selection, thereby improving model accuracy and efficiency while mitigating the risk of overfitting.

No study has investigated an Xgboost-based classification model using EEG data for patients with dementia. Previous studies have reported that Xgboost, using combined biomarkers such as genes, MRI, PET scans, and neuropsychological measurements, was effective in detecting patients with dementia, mild cognitive impairment (MCI), and normal controls (NCs)^{24,25}. The Xgboost model achieved a classification accuracy of 87.57% when incorporating weighted imbalance to balance the uneven sample sizes²⁶. In very small datasets, Xgboost can provide reasonable classification performance if the parameters are tuned appropriately²⁷.

The current study explored a machine learning model using Xgboost-based EEG biomarkers to distinguish between patients with dementia and NCs. In this study, an optimized ensemble tree-based learning model and RFECV were applied to establish an efficient and precise classification model for detecting dementia. Additionally, the RFECV-Xgboost model was compared with the RFECV-Random Forest (RF) model to validate its classification performance.

Results

Demographic characteristics

Results of demographic characteristics are presented in Table 1. A significant difference in age was found between patients with dementia and NCs, with patients with dementia being older than NCs ($t=5.70, p<0.001$). Age was negatively correlated with Mini-Mental Status Exam (MMSE) scores in the study population ($r=-0.53, p<0.001$). Age was positively correlated with Clinical Dementia Rating (CDR) scores ($r=0.38, p<0.001$). MMSE scores were negatively correlated with CDR scores ($r=-0.70, p<0.001$), after controlling for age. The chi-square test showed no significant association between study group and sex ($p=0.825$). A significant difference in MMSE scores was found between patients with dementia and NCs ($t=11.32, p<0.001$). In CDR scores, a significant difference was found ($t=4.28, P<0.001$). There was also a significant difference in formal education levels ($t=3.33, p=0.002$). Additionally, patients with dementia were further divided into mild dementia and moderate-severe dementia groups. Significant differences were observed in age ($t=2.76, p=0.010$), MMSE scores ($t=4.69, p=0.005$), and CDR scores ($t=3.70, P=0.012$). Patients with moderate-severe dementia were older than those with mild dementia, and patients with mild dementia had higher MMSE scores than those with moderate-severe dementia. The CDR scores of patients with moderate-severe dementia were higher than those of mild dementia. The results of the subgroup analysis were not considered major findings.

Statistical comparison based on spectral power

Table 2 presents the statistical comparisons of EEG spectral values between patients with dementia and NCs. Compared to NCs, patients with dementia showed a significant decrease in EEG power for several indices ($F_{(1,80)}=8.47, *p<0.001, \eta^2=0.75$): *PF1 ($F_{(1,80)}=146.73, \eta^2=0.65$), *PF2 ($F_{(1,80)}=137.98, \eta^2=0.63$), *CH_A/T ($F_{(1,80)}=14.16, \eta^2=0.15$), *CH_A/BL ($F_{(1,80)}=13.49, \eta^2=0.14$), *A1/T1 ($F_{(1,80)}=30.81, \eta^2=0.28$), *A2/T2 ($F_{(1,80)}=29.50, \eta^2=0.27$), *A1 ($F_{(1,80)}=47.58, \eta^2=0.37$), *A2 ($F_{(1,80)}=41.25, \eta^2=0.34$), *A1/BL1 ($F_{(1,80)}=21.23, \eta^2=0.21$), and *A2/BL2 ($F_{(1,80)}=11.81, \eta^2=0.13$). Conversely, there was a significant increase for *T1 ($F_{(1,80)}=29.62, \eta^2=0.27$) and *T2 ($F_{(1,80)}=25.75, \eta^2=0.24$) in patients with dementia.

Classification results based on spectral power

Table 3 shows the classification model performance and the ranking of the initial 24 features. Figure 1 displays the ROC curve panels for the initial 24 features and the RFECV-selected features. A total of 24 initial EEG features

	Dementia($n=29$) (MMSE < 24)	Normal($n=54$) (MMSE ≥ 24)	Statistics
Age(M \pm SD)	74.24 \pm 7.20	64.15 \pm 7.95	$p<0.001$
Sex(m/f)	17/12	33/21	$p=0.825$
Education, n(M \pm SD)	14(7.71 \pm 4.34)	38(11.37 \pm 3.17)	$p=0.002$
MMSE(M \pm SD)	19.97 \pm 3.33	27.46 \pm 1.73	$p<0.001$
CDR(M \pm SD)	0.83 \pm 0.47	0.44 \pm 0.16	$P<0.001$
	Moderate-Severe Dementia ($n=6$) (MMSE < 20)	Mild Dementia ($n=23$) (20 \leq MMSE < 24)	
Age(M \pm SD)	78.17 \pm 1.94	73.22 \pm 7.73	$p=0.010$
Sex(m/f)	4-Feb	15/7	
Education, n(M \pm SD)	4(4.75 \pm 3.40)	10(8.90 \pm 4.23)	$p=0.108$
MMSE(M \pm SD)	14.50 \pm 3.56)	21.39 \pm 0.99	$p=0.005$
CDR(M \pm SD)	1.50 \pm 0.55	0.65 \pm 0.24	$P=0.012$

Table 1. Demographic characteristics of study participants. MMSE, Mini-Mental Status Exam; CDR, Clinical Dementia Rating. M, mean; SD, standard deviation.

	Dementia(<i>n</i> = 29)	Normal(<i>n</i> = 54)	Statistics
	Mean \pm SD		
PF1	5.91 \pm 1.28	8.90 \pm 0.49	* <i>p</i> < 0.001, η^2 = 0.648
PF2	6.20 \pm 1.19	8.90 \pm 0.48	* <i>p</i> < 0.001, η^2 = 0.634
CH_A/T	0.87 \pm 0.17	1.25 \pm 0.39	* <i>p</i> < 0.001, η^2 = 0.152
CH_A/BL	1.10 \pm 0.21	1.49 \pm 0.43	* <i>p</i> < 0.001, η^2 = 0.147
A1/T1	0.59 \pm 0.12	0.97 \pm 0.25	* <i>p</i> < 0.001, η^2 = 0.278
A2/T2	0.62 \pm 0.14	0.94 \pm 0.20	* <i>p</i> < 0.001, η^2 = 0.273
T1	0.51 \pm 0.06	0.41 \pm 0.05	* <i>p</i> < 0.001, η^2 = 0.270
T2	0.50 \pm 0.06	0.41 \pm 0.04	* <i>p</i> < 0.001, η^2 = 0.245
A1	0.29 \pm 0.03	0.39 \pm 0.05	* <i>p</i> < 0.001, η^2 = 0.377
A2	0.30 \pm 0.03	0.38 \pm 0.04	* <i>p</i> < 0.001, η^2 = 0.349
A1/BL1	2.03 \pm 0.30	2.73 \pm 0.57	* <i>p</i> < 0.001, η^2 = 0.223
A2/BL2	2.12 \pm 0.33	2.63 \pm 0.55	* <i>p</i> < 0.001, η^2 = 0.135
CH_T	0.43 \pm 0.24	0.46 \pm 0.20	<i>p</i> = 0.329, η^2 = 0.012
CH_A	0.37 \pm 0.22	0.53 \pm 0.19	<i>p</i> = 0.005, η^2 = 0.095
CH_BL	0.34 \pm 0.20	0.39 \pm 0.19	<i>p</i> = 0.301, η^2 = 0.014
CH_BH	0.36 \pm 0.22	0.39 \pm 0.18	<i>p</i> = 0.362, η^2 = 0.011
CH_T/BL	1.29 \pm 0.26	1.27 \pm 0.52	<i>p</i> = 0.572, η^2 = 0.004
T1/BL1	3.66 \pm 1.09	2.87 \pm 0.54	<i>p</i> = 0.004, η^2 = 0.100
T2/BL2	3.61 \pm 1.12	2.84 \pm 0.52	<i>p</i> = 0.004, η^2 = 0.100
BL1	0.15 \pm 0.03	0.15 \pm 0.02	<i>p</i> = 0.631, η^2 = 0.003
BL2	0.15 \pm 0.03	0.15 \pm 0.02	<i>p</i> = 0.870, η^2 = 0.0003
BH1	0.06 \pm 0.02	0.05 \pm 0.01	<i>p</i> = 0.126, η^2 = 0.029
BH2	0.05 \pm 0.02	0.05 \pm 0.01	<i>p</i> = 0.168, η^2 = 0.024

Table 2. Comparison between dementia and normal controls (MANCOVA). *Adjusted *P* < 0.002, 0.05/23. A/T, alpha to theta ratio; A/BL, alpha to low-beta ratio; T/BL, theta to low-beta ratio; BH, high-beta; CH, coherence; 1, left; 2, right; PF, peak frequency.

were input into the classification model for RFECV using Xgboost. The classification performance with the initial 24 features resulted in a balanced accuracy of 94.12%, sensitivity of 95.82%, specificity of 92.42%, F1 score of 0.92, and an AUC of 0.97. Through RFECV, the final selected feature was PF1. The classification performance with the selected feature the PF1 achieved a balanced accuracy of 97.05%, sensitivity of 97.96%, specificity of 96.14%, F1 score of 0.96, and an AUC of 0.97. For age, the balanced accuracy was 66.15%, sensitivity was 71.27%, specificity was 61.03%, F1 score was 0.54, and AUC was 0.66. Additionally, RFECV-RF showed lower classification performance than RFECV-Xgboost. As a result, RFECV-RF achieved a classification accuracy of 93.28%. The selected features in RF were PF1, PF2, and A2 (Table 4).

Correlations of EEG measures with MMSE and CDR

EEG measures were correlated with MMSE scores in all participants. The results of the correlations are displayed in Fig. 2. Positive correlations were found for *PF1 (*r* = 0.66), *PF2 (*r* = 0.65), *CH_A/T (*r* = 0.34), *A1/T1 (*r* = 0.46), *A2/T2 (*r* = 0.51), *A1 (*r* = 0.55), *A2 (*r* = 0.58), and *A1/BL1 (*r* = 0.38) (adjusted **p* < 0.002). Negative correlations were found for *T1/BL1 (*r* = -0.37), *T2/BL2 (*r* = -0.39), *T1 (*r* = -0.49), and *T2 (*r* = -0.52) (adjusted **p* < 0.002). Additionally, EEGs were correlated with CDR scores in all participants. Negative correlations were found for *PF1 (*r* = -0.38), *PF2 (*r* = -0.39), *A1/T1 (*r* = -0.52), *A2/T2 (*r* = -0.54), *A1 (*r* = -0.54), and *A2 (*r* = -0.55) (adjusted **p* < 0.002). Positive correlations were found for *T1/BL1 (*r* = 0.51), *T2/BL2 (*r* = 0.49), *T1 (*r* = 0.60), and *T2 (*r* = 0.59) (adjusted **p* < 0.002).

Discussion

The present study explored the distinguishable two-channel EEG biomarkers using tree ensemble learning model in patients with dementia and NCs. As summarize the results those are as follows: 1) In statistical comparison, patients with dementia showed decreased activities in PF1, PF2, CH_A/T, CH_A/BL, A1/T1, A2/T2, A1, A2, A1/BL1, and A2/BL2 as well as increase in T1 and T2.

2) Our main findings were the results on machine learning. Initial 24 features were ranked by RFECV with Xgboost. PF1 in EEGs was selected as the highest ranked feature. The balanced classification accuracy of PF1 was 97.05% and that of 24 features was 94.12% between patients with dementia and NCs. To identify the effect of age on classification model, age was inputted as a feature. The balanced accuracy in age was 66.15% which was ranked 24th of 24.

3) The correlations of EEGs with MMSE and CDR score were found in all participants. The MMSE was positively correlated with PF1, PF2, CH_A/T, A1/T1, A2/T2, A1, A2, and A1/BL1. The MMSE was negatively

Rank no.	Feature	Dementia(<i>n</i> = 29)	Normal(<i>n</i> = 54)	Statistics	Classification Performance
		Mean \pm SD			
1	PF1	5.91 \pm 1.28	8.90 \pm 0.49	* <i>p</i> < 0.001	Initial 24-features Balanced accuracy: 94.12% Sensitivity: 95.82% Specificity: 92.42% F1 score: 0.92 AUC: 0.97
2	A1/T1	0.59 \pm 0.12	0.97 \pm 0.25	* <i>p</i> < 0.001	
3	A2/T2	0.62 \pm 0.14	0.94 \pm 0.20	* <i>p</i> < 0.001	
4	PF2	6.20 \pm 1.19	8.90 \pm 0.48	* <i>p</i> < 0.001	
5	BH1	0.06 \pm 0.02	0.05 \pm 0.01	<i>p</i> = 0.126	
6	T1/BL1	3.66 \pm 1.09	2.87 \pm 0.54	<i>p</i> = 0.004	
7	CH_BH	0.36 \pm 0.22	0.39 \pm 0.18	<i>p</i> = 0.362	
8	A1/BL1	2.03 \pm 0.30	2.73 \pm 0.57	* <i>p</i> < 0.001	
9	T2	0.50 \pm 0.06	0.41 \pm 0.04	* <i>p</i> < 0.001	
10	BL2	0.15 \pm 0.03	0.15 \pm 0.02	<i>p</i> = 0.870	
11	A1	0.29 \pm 0.03	0.39 \pm 0.05	* <i>p</i> < 0.001	
12	CH_T	0.43 \pm 0.24	0.46 \pm 0.20	<i>p</i> = 0.329	
13	CH_A/BL	1.10 \pm 0.21	1.49 \pm 0.43	* <i>p</i> < 0.001	
14	CH_T/BL	1.29 \pm 0.26	1.27 \pm 0.52	<i>p</i> = 0.572	
15	A2/BL2	2.12 \pm 0.33	2.63 \pm 0.55	* <i>p</i> < 0.001	
16	BH2	0.05 \pm 0.02	0.05 \pm 0.01	<i>p</i> = 0.168	
17	T2/BL2	3.61 \pm 1.12	2.84 \pm 0.52	<i>p</i> = 0.004	
18	A2	0.30 \pm 0.03	0.38 \pm 0.04	* <i>p</i> < 0.001	
19	T1	0.51 \pm 0.06	0.41 \pm 0.05	* <i>p</i> < 0.001	
20	CH_BL	0.34 \pm 0.20	0.39 \pm 0.19	<i>p</i> = 0.301	
21	BL1	0.15 \pm 0.03	0.15 \pm 0.02	<i>p</i> = 0.631	
22	CH_A/T	0.87 \pm 0.17	1.25 \pm 0.39	* <i>p</i> < 0.001	
23	CH_A	0.37 \pm 0.22	0.53 \pm 0.19	<i>p</i> = 0.005	
24	Age	74.24 \pm 7.20	64.15 \pm 7.95	* <i>p</i> < 0.001	
RFECV-Selected Feature in Xgboost					
	PF1	5.91 \pm 1.28	8.90 \pm 0.49	* <i>p</i> < 0.001	Balanced accuracy: 97.05% Sensitivity: 97.96% Specificity: 96.14% F1 score: 0.96 AUC: 0.97

Table 3. Classification model and rank of features in RFECV with Xgboost. A/T, alpha to theta ratio; A/BL, alpha to low-beta ratio; T/BL, theta to low-beta ratio; BH, high-beta; CH, coherence; 1, left; 2, right; PF, peak frequency.

correlated with T1/BL1, T2/BL2, T1, and T2. The CDR was negatively correlated with PF1, PF2, A1/T1, A2/T2, A1, and A2. The CDR was positively correlated with T1/BL1, T2/BL2, T1, and T2.

A decrease in PF is associated with memory impairment in patients with dementia²⁸. In our study, patients with AD had a PF of 5.91 \pm 1.28, while NCs had a PF of 8.90 \pm 0.49. The PF in AD patients was observed within the theta frequency range, whereas in NCs, it was within the alpha frequency range. PF is an intuitive measure that identifies the most representative frequency within a given band (Supplementary Figure). According to previous study, PF is a useful indicator of the awake state, reflecting levels of consciousness as well as the transition from the rise to the fall of spectral power²⁹. It is used to distinguish neural deficits between patients with AD and frontotemporal lobar degeneration, and neural changes are reflected in the correlation between PF and MMSE scores³⁰. Another study reported that AD patients showed a lower occipital peak frequency than elderly controls, with the exception of cases where the CDR score was 0.5³¹. In our study, 48 NCs had a CDR score of 0.5, while the remaining 6 had a score of 0.0. This suggests the possibility that patients with a CDR score of 0.5 may show no EEG changes and that individuals with a CDR score of 0.5 may not progress to dementia. Alpha frequency plays a role in sensory gating during pre-attentive information processing, which is critical in the resting-state default mode network^{32,33}. Patients with dementia show malfunctions in attention and working memory as resting-state alpha is decreased³⁴. Alpha to beta ratio could indicate a better cognitive performance which is reduced in patients AD³⁵. Our findings were that compared to NCs, alpha to theta ratio was reduced in patients with dementia. A Reduction in A/T and CH_A/T is also indicative for dementia, reflecting decreased alpha activity relative to theta as well as beta. Furthermore, PF is the most distinctive biomarker of dementia, and it represents the most prominent frequency power between alpha and theta.

Our primary finding underscores that a tree ensemble-based classification model employing Xgboost and RFECV exhibited the highest performance score when distinguishing between patients and NCs. Remarkably, the final selected feature, PF1, achieved a balanced accuracy of 97.05%. Notably, the initial set of 24 features demonstrated reasonable performance (94.12%), with one particular feature proving exceptionally effective. Additionally, compared to the baseline model using RF, the Xgboost model demonstrated better classification performance. This suggests the potential to achieve optimal classification performance using a single selected

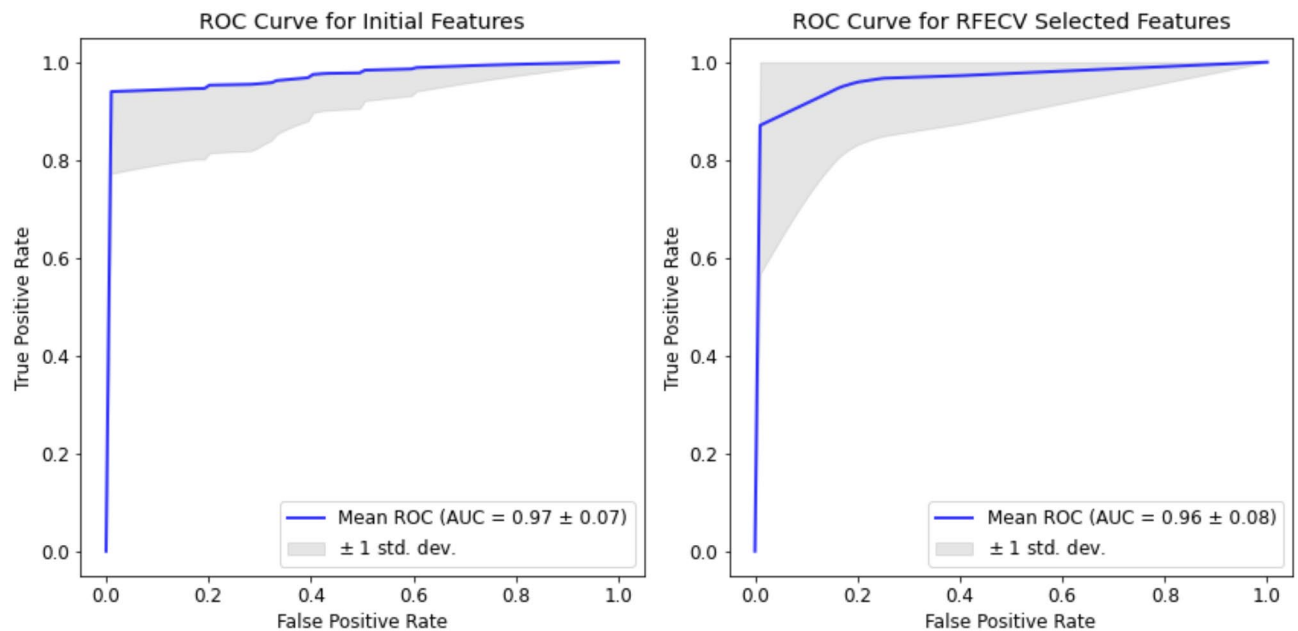


Fig. 1. ROC curve panels in EEG features in Xgboost classification model.

EEG feature, which could aid in dementia diagnosis. Furthermore, this approach yielded superior performance compared to the biological age. Although the age difference was statistically adjusted using MANCOVA, we acknowledge that age may still influence EEG results. However, in our classification model, age was found to have the lowest importance among the input features, suggesting that its impact on classification outcomes is minimal. Previously, Xgboost utilizing MRI and PET data demonstrated excellent diagnostic performance for dementia³⁶. In our study, the feature selection technique, RFECV combined with Xgboost, achieved nearly 100% accuracy using only two-channel frontal EEG data, employing weighted balancing to prevent overfitting. Despite the increased computational load, RFECV would play a crucial role in selecting the optimal EEG features for diagnosing dementia.

Previous studies reported that cognitive functions estimating by MMSE associated with frontal EEG activity in both senior people and patients with dementia^{37,38}. Especially, alpha and beta frequency were correlated with MMSE score in both patients with AD and NCs³⁹. PF was also correlated to MMSE in elderly people³⁸. Our results imply that correlations between EEG and MMSE scores are reproducible in both patients and NCs. Therefore, increases in alpha, beta, and PF activity would be beneficial for aligning with MMSE scores to assess cognitive functions in dementia. Conversely, decreases in theta activity correlated with MMSE would also be useful for estimating cognitive functions.

Conclusions

The present study identified a novel approach utilizing Xgboost with RFECV-based feature selection from data captured by a frontal two-channel device for detecting dementia. Additionally, our concerns have addressed smaller sample sizes and imbalanced class. We aimed to mitigate these challenges through assigning weights to the imbalanced class. However, these limitations should be acknowledged and addressed in future studies. In particular, the limited sample size may impact the generalizability of the findings. Therefore, validating the model with larger and more diverse AD populations is essential to enhance its reliability and clinical applicability. In conclusion, the Xgboost with RFECV model using two-channel EEG data holds significant promise in assisting with dementia diagnosis.

Materials and methods

Participants

Eighty-three outpatients voluntarily consented to participate in the study at a university hospital. Twenty-nine patients were diagnosed with dementia, showing mild impairments in memory, executive function, attention, and general cognition. The remaining 54 participants served as NCs recruited from the general medicine departments of the same hospital. Inclusion criteria included being adults aged 18 years and older, capable of communication, and providing voluntary consent. It was determined that various types of dementia such as Dementia with Lewy Bodies (DLB), Parkinson's disease dementia (PDD), and Frontotemporal Dementia (FTD) could interfere EEG analysis due to differences in pathological findings and brain invasion sites compared to Alzheimer's dementia. Therefore, only Alzheimer's dementia patients were enrolled in this study. For the diagnosis of AD, brain MRI was performed in patients with a score of less than 24 on the MMSE screening to identify and exclude vascular dementia, and brain atrophy and white matter hyperintensity were confirmed. Afterwards, the Seoul Neuropsychological Screening Battery (SNSB), a neuropsychological battery developed

Rank no.	Feature	Dementia(<i>n</i> = 29)	Normal(<i>n</i> = 54)	Statistics	Classification performance
		Mean \pm SD			
1	PF1	5.91 \pm 1.28	8.90 \pm 0.49	* <i>p</i> < 0.001	Initial 24-features Balanced accuracy: 91.86% Sensitivity: 94.64% Specificity: 89.07% F1 score: 0.87 AUC: 0.92
1	PF2	6.20 \pm 1.19	8.90 \pm 0.48	* <i>p</i> < 0.001	
1	A2	0.30 \pm 0.03	0.38 \pm 0.04	* <i>p</i> < 0.001	
2	A1	0.29 \pm 0.03	0.39 \pm 0.05	* <i>p</i> < 0.001	
3	A2/T2	0.62 \pm 0.14	0.94 \pm 0.20	* <i>p</i> < 0.001	
4	A1/T1	0.59 \pm 0.12	0.97 \pm 0.25	* <i>p</i> < 0.001	
5	T2	0.50 \pm 0.06	0.41 \pm 0.04	* <i>p</i> < 0.001	
6	BH1	0.06 \pm 0.02	0.05 \pm 0.01	<i>p</i> = 0.126	
7	A1/BL1	2.03 \pm 0.30	2.73 \pm 0.57	* <i>p</i> < 0.001	
8	CH_T/BL	1.29 \pm 0.26	1.27 \pm 0.52	<i>p</i> = 0.572	
9	BH2	0.05 \pm 0.02	0.05 \pm 0.01	<i>p</i> = 0.168	
10	T1	0.51 \pm 0.06	0.41 \pm 0.05	* <i>p</i> < 0.001	
11	CH_A/T	0.87 \pm 0.17	1.25 \pm 0.39	* <i>p</i> < 0.001	
12	CH_BH	0.36 \pm 0.22	0.39 \pm 0.18	<i>p</i> = 0.362	
13	Age	74.24 \pm 7.20	64.15 \pm 7.95	* <i>p</i> < 0.001	
14	T2/BL2	3.61 \pm 1.12	2.84 \pm 0.52	<i>p</i> = 0.004	
15	BL2	0.15 \pm 0.03	0.15 \pm 0.02	<i>p</i> = 0.870	
16	CH_BL	0.34 \pm 0.20	0.39 \pm 0.19	<i>p</i> = 0.301	
17	CH_A	0.37 \pm 0.22	0.53 \pm 0.19	<i>p</i> = 0.005	
18	CH_A/BL	1.10 \pm 0.21	1.49 \pm 0.43	* <i>p</i> < 0.001	
19	T1/BL1	3.66 \pm 1.09	2.87 \pm 0.54	<i>p</i> = 0.004	
20	A2/BL2	2.12 \pm 0.33	2.63 \pm 0.55	* <i>p</i> < 0.001	
21	CH_T	0.43 \pm 0.24	0.46 \pm 0.20	<i>p</i> = 0.329	
22	BL1	0.15 \pm 0.03	0.15 \pm 0.02	<i>p</i> = 0.631	
RFECV-Selected Feature in RF					
	PF1	5.91 \pm 1.28	8.90 \pm 0.49	* <i>p</i> < 0.001	Balanced accuracy: 93.28% Sensitivity: 97.96% Specificity: 88.60% F1 score: 0.90 AUC: 0.93
	PF2	6.20 \pm 1.19	8.90 \pm 0.48	* <i>p</i> < 0.001	
	A2	0.30 \pm 0.03	0.38 \pm 0.04	* <i>p</i> < 0.001	

Table 4. Classification model and rank of features in RFECV with RF. A/T, alpha to theta ratio; A/BL, alpha to low-beta ratio; T/BL, theta to low-beta ratio; BH, high-beta; CH, coherence; 1, left; 2, right; PF, peak frequency.

in Korea, was conducted⁴⁰. Patients primarily exhibited impairments in memory domains, such as immediate and delayed recall tests, as well as deficits in language and visuospatial function, leading to the diagnosis of AD and their enrollment in the study. Eighteen patients underwent amyloid PET scans, which confirmed their AD diagnosis. The remaining patients were unable to undergo amyloid PET due to financial constraints. A total of 29 dementia patients were enrolled, with outpatient follow-up periods ranging from 2 years and 3 months to 8 years and 5 months. The average duration of dementia was 4 years and 2 months. Rapidly progressive dementia was not included, as only Alzheimer's dementia was included, excluding other types of dementia. All participants underwent the CDR assessment. A higher CDR score increases the probability of a dementia and mild cognitive impairment⁴¹. Individuals with severe physical or mental health conditions such as stroke, brain injury, intellectual disability, or psychiatric disorders requiring medication were excluded. Participants using sleeping pills, antidepressants, antipsychotics, or sedatives—due to their potential to cause significant EEG slowing, which interferes with analysis—were also excluded. The mean age of patients with dementia was 74.24 \pm 7.20 years, with 17 males and 12 females. For NCs, the mean age was 64.15 \pm 7.95 years, with 33 males and 21 females. Among the 29 patients with dementia, the mean formal education duration was 7.71 \pm 4.34 years, while among the 54 NCs, it was 11.37 \pm 3.17 years. Formal education duration information was missing for some participants (patients: 15 of 29 and NCs: 16 of 54). All participants completed the MMSE to evaluate cognitive ability. A score below 24 on the MMSE indicated dementia, further classified into mild dementia (<24) and moderate-severe dementia (<20). Subgroup analysis of dementia groups was limited due to the smaller sample size (Table 1).

The study was approved by the International Review Board (IRB) of International St. Mary's Hospital (IRB Number: IS21OISE0035), Incheon, South Korea. Written informed consent was obtained from all participants.

EEG recording and preprocessing

Participants were seated in a sound-attenuated room and instructed to remain still and quiet in a chair with their eyes closed. EEG recording lasted 180 s using the Neuroharmony S, a 2-channel EEG device (PANAXTOS Co. Ltd, Seoul, South Korea). Gold-coated dry electrodes were placed on the prefrontal area at fp1 and fp2, with a reference electrode on the left ear lobe and the ground on fpz. The sampling frequency was set to 250 Hz, and

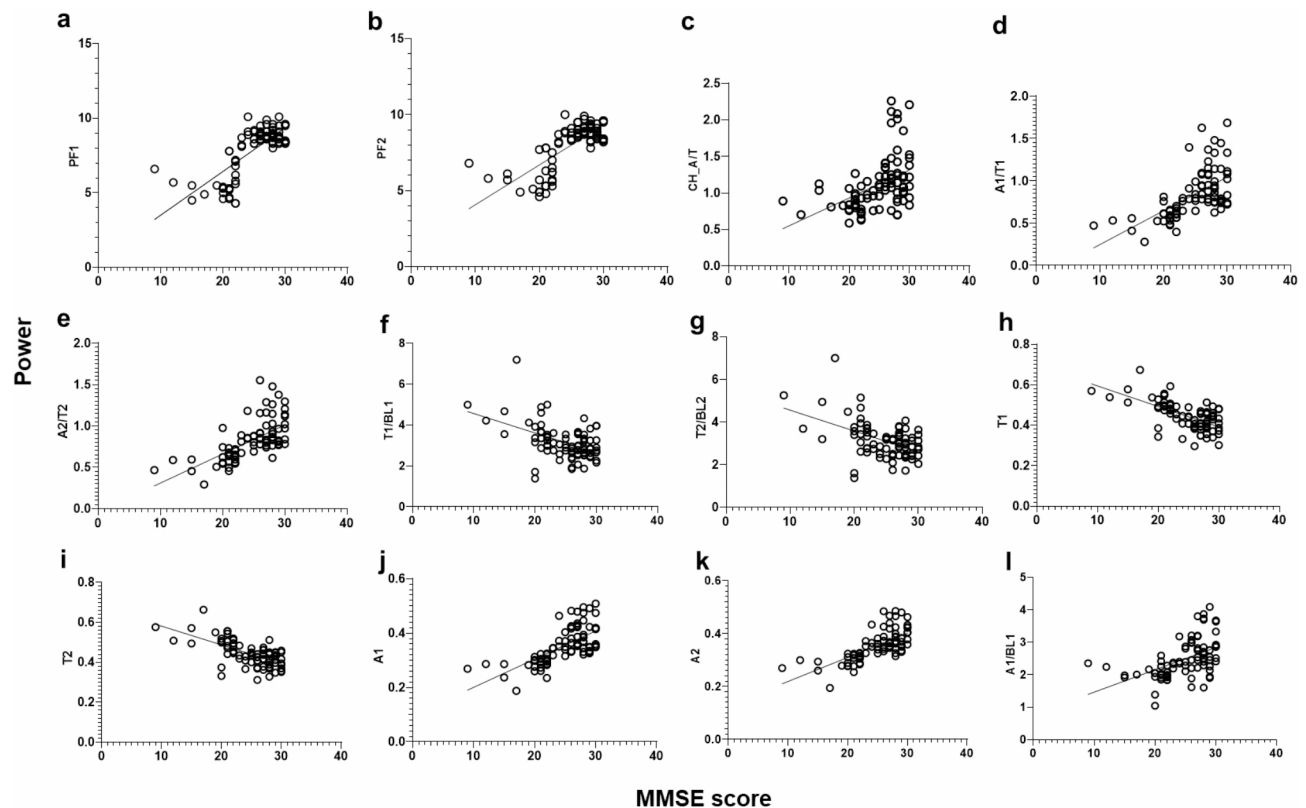


Fig. 2. Partial correlations among EEG features and MMSE in all participants.

an expert, not affiliated with the study, conducted the EEG recording. A high-pass filter at 3 Hz was applied to the data.

Quantitative EEG analysis

The EEG data were recorded at 250 Hz and segmented into 250-millisecond epochs, with a total of 40 s used for analysis. Data were processed using fast Fourier transformation (FFT)⁴². FFT was applied to 40 segments, each lasting 1 s, and their averaged values were computed. Absolute band frequencies were extracted across theta (T, 4.0–7.9 Hz), alpha (A, 8.0–12.9 Hz), low-beta (BL, 13.0–20.9 Hz), and high-beta (BH, 21.0–30.9 Hz). Peak frequencies (PF) were calculated as the frequency where the highest power is observed within the frequency range of 4.0 to 12.9 Hz (Supplementary Figure). Coherence (CH) between the two EEG channels (left-sided: 1 and right-sided: 2) was computed as the squared magnitude of their cross-spectral density (CSD) divided by the product of their individual auto-spectral densities (ASD). This calculation provides a measure of the strength of frequency-specific connectivity between the two channels.

$$Coherence(f) = \frac{|CSD_{12}(f)|^2}{ASD_1(f) \cdot ASD_2(f)}$$

Where: $CSD_{12}(f)$ is the cross-spectral density between channel 1 and channel 2 at frequency f . $ASD_1(f)$ is the auto-spectral density of channel 1 at frequency f . $ASD_2(f)$ is the auto-spectral density of channel 2 at frequency f . $|CSD_{12}(f)|^2$ is the squared magnitude of the cross-spectral density between two channels. This coherence measure indicates the extent of linear correlation between the two channels at a specific frequency. The coherence values range from 0 to 1, where a value near 1 signifies a strong correlation, and a value near 0 signifies a weak or no correlation. The ratio between various frequencies was computed as follows: A to T (A/T), A to BL (A/BL), T to BL (T/BL), CH_A to CH_T (CH_A/T), CH_A to BL (CH_A/BL), and CH_T to BL (CH_T/BL).

Statistical analysis

Pearson's chi-square test was conducted to assess the association between group (patients with dementia vs. NCs) and sex. Age, education, MMSE, and CDR scores were compared between patients with dementia and NCs, as well as between patients with mild dementia and those with moderate-severe dementia. Multivariate analysis of covariance (MANCOVA) was used to compare EEG measures between patients with dementia and NCs, with age included as a covariate. Partial correlation analysis was performed to examine the relationship among EEG measures, and MMSE, and CDR scores, controlling for age. Subgroup analysis comparing patients with mild dementia and those with moderate-severe dementia was only conducted in demographic analyses. The significance level was set at 0.05 with a two-tailed. To account for multiple comparisons, the Bonferroni

correction was applied, adjusting the significance threshold to <0.002 . Effect sizes were calculated and reported using eta-squared (η^2).

Feature selection and classification

Feature selection

RFECV⁴³, an iterative method that selects the optimal subset of features based on model performance metrics. An Xgboost classifier served as the base estimator for RFECV. The technique included nested cross-validation to robustly identify the most discriminative features for classification. RF was used to validate the Xgboost model for comparison.

Classifier model

An Xgboost classifier, which is decision tree-based and ensembled, was chosen for its capability to effectively handle complex relationships, making it well-suited for classifying between two distinct groups. Model configuration included parameters optimized for the dataset. Class weights (AD: 1.86 and NC: 0.537) were adjusted to address class imbalance in the dataset, ensuring balanced model training. The model was designed to give 1.86 times more importance to AD samples during training, while NC is assigned a lower weight of 0.537. In feature selection and classifier model configuration, the evaluation metric used was a log-loss for binary classification. The histogram-based method, derived features from time-frequency, was used for constructing trees, with the number of boosting rounds set to 50. The RF classifier was also utilized as a baseline model for comparison. The RF model was trained using 50 estimators, with log-loss used as the evaluation metric for classification.

Evaluation metrics

Model performance was assessed using several metrics including balanced accuracy, which considers both sensitivity and specificity, making it suitable for imbalanced datasets. Sensitivity (true positive rate) and specificity (true negative rate) were computed to evaluate the model's ability to accurately predict positive and negative instances. The F1 Score, which is the weighted average of precision and recall, provided a balanced measure of the classifier's performance. Additionally, the area under the receiver operating characteristic curve (AUC-ROC) indicated the classifier's discriminative ability between classes, with higher values indicating better performance.

Cross-Validation

To ensure robustness of the results, repeated K-fold cross-validation was employed. The dataset was divided into 10-folds and repeated 10-times to reliably estimate model performance using EEG data between two classes. Each iteration involved training the model on a subset of data and evaluating its performance on held-out data.

Data availability

The datasets used and/or analyzed during the current study available from the corresponding author on reasonable request.

Received: 23 July 2024; Accepted: 7 March 2025

Published online: 03 April 2025

References

- Nichols, E. et al. Estimation of the global prevalence of dementia in 2019 and forecasted prevalence in 2050: an analysis for the global burden of disease study 2019. *Lancet Public Health*. **7**, e105–e125. [https://doi.org/10.1016/S2468-2667\(21\)00249-8](https://doi.org/10.1016/S2468-2667(21)00249-8) (2022).
- Jang, J. W. et al. Prevalence and incidence of dementia in South Korea: A nationwide analysis of the National health insurance service senior cohort. *J. Clin. Neurol. (Seoul Korea)*. **17**, 249–256. <https://doi.org/10.3988/jcn.2021.17.2.249> (2021).
- Ready, R. E. & Ott, B. R. Quality of life measures for dementia. *Health Qual. Life Outcomes*. **1** <https://doi.org/10.1186/1477-7525-1-11> (2003).
- Rasmussen, J. & Langerman, H. Alzheimer's Disease - Why we need early diagnosis. *Degenerative Neurol. Neuromuscul. Disease*. **9**, 123–130. <https://doi.org/10.2147/dnnd.S228939> (2019).
- Lewczuk, P. et al. Cerebrospinal fluid and blood biomarkers for neurodegenerative dementias: an update of the consensus of the task force on biological markers in psychiatry of the world federation of societies of biological psychiatry. *World J. Biol. Psychiatry: Official J. World Federation Soc. Biol. Psychiatry*. **19**, 244–328. <https://doi.org/10.1080/15622975.2017.1375556> (2018).
- Lombardi, G. et al. Structural magnetic resonance imaging for the early diagnosis of dementia due to Alzheimer's disease in people with mild cognitive impairment. *Cochrane Database Syst. Rev.* **3**, Cd009628. <https://doi.org/10.1002/14651858.CD009628.pub2> (2020).
- Chouliaras, L. & O'Brien, J. T. The use of neuroimaging techniques in the early and differential diagnosis of dementia. *Mol. Psychiatry*. **28**, 4084–4097. <https://doi.org/10.1038/s41380-023-02215-8> (2023).
- Arvanitakis, Z., Shah, R. C. & Bennett, D. A. Diagnosis and Management of Dementia: Review. *JAMA* **322**, 1589–1599. <https://doi.org/10.1001/jama.2019.4782> (2019).
- Knopman, D. S. et al. Practice parameter: diagnosis of dementia (an evidence-based review). **56**, 1143–1153, doi: (2001). <https://doi.org/10.1212/WNL.56.9.1143>
- Brown, C. W., Chen, H. Y. & Panegyres, P. K. Electroencephalography in young onset dementia. *BMC Neurol.* **23**, 202. <https://doi.org/10.1186/s12883-023-03248-w> (2023).
- Al-Qazzaz, N. K. et al. Role of EEG as Biomarker in the Early Detection and Classification of Dementia. 906038, (2014). <https://doi.org/10.1155/2014/906038> (2014).
- Kopčanová, M. et al. Resting-state EEG signatures of Alzheimer's disease are driven by periodic but not aperiodic changes. *BioRxiv: Preprint Serv. Biology*. <https://doi.org/10.1101/2023.06.11.544491> (2023).
- Musaev, C. S. et al. EEG Theta power is an early marker of cognitive decline in dementia due to Alzheimer's disease. *J. Alzheimer's Disease: JAD*. **64**, 1359–1371. <https://doi.org/10.3233/jad-180300> (2018).

14. Schumacher, J. et al. EEG alpha reactivity and cholinergic system integrity in lewy body dementia and Alzheimer's disease. *Alzheimers Res. Ther.* **12**, 46. <https://doi.org/10.1186/s13195-020-00613-6> (2020).
15. van der Zande, J. J. et al. Diagnostic and prognostic value of EEG in prodromal dementia with lewy bodies. *Neurology* **95**, e662–e670. <https://doi.org/10.1212/wnl.0000000000009977> (2020).
16. Gola, M., Magnuski, M., Szumska, I. & Wróbel, A. EEG beta band activity is related to attention and attentional deficits in the visual performance of elderly subjects. *Int. J. Psychophysiology: Official J. Int. Organ. Psychophysiol.* **89**, 334–341. <https://doi.org/10.1016/j.ijpsycho.2013.05.007> (2013).
17. Aderinwale, A. et al. Two-channel EEG based diagnosis of panic disorder and major depressive disorder using machine learning and non-linear dynamical methods. *Psychiatry Res. Neuroimaging* **332**, 111641. <https://doi.org/10.1016/j.psychres.2023.111641> (2023).
18. Jang, K. I. et al. Increased beta power in the bereaved families of the Sewol ferry disaster: A Paradoxical compensatory phenomenon? A two-channel electroencephalography study. *J. Neuropsychiatry Clin. Neurosci.* **71**, 759–768. <https://doi.org/10.1111/pcn.12546> (2017).
19. Hu, L. & Li, L. Using Tree-Based machine learning for health studies: literature review and case series. *Int. J. Environ. Res. Public Health* **19**. <https://doi.org/10.3390/ijerph192316080> (2022).
20. Nayarissari, A. et al. Artificial intelligence, big data and machine learning approaches in precision medicine & drug discovery. *Curr. Drug Targets* **22**, 631–655. <https://doi.org/10.2174/1389450122999210104205732> (2021).
21. Chen, T. & Guestrin, C. XGBoost: A Scalable Tree Boosting System. (2016).
22. Mustaqim, A. Z., Adi, S., Pristyanto, Y. & Astuti, Y. in *2021 International Conference on Artificial Intelligence and Computer Science Technology (ICAICST)*. 270–275.
23. Misra, P. & Singh, A. Improving the Classification Accuracy using Recursive Feature Elimination with Cross-Validation. *International Journal on Emerging Technologies* **11**(3), 659–665 (2020).
24. Stamate, D. et al. A metabolite-based machine learning approach to diagnose alzheimer-type dementia in blood: results from the European medical information framework for alzheimer disease biomarker discovery cohort. *Alzheimer's Dement. (New York N Y)* **5**, 933–938. <https://doi.org/10.1016/j.trci.2019.11.001> (2019).
25. Danso, S. O., Zeng, Z., Muniz-Terrera, G. & Ritchie, C. W. Developing an explainable machine learning-Based personalised dementia risk prediction model: A transfer learning approach with ensemble learning algorithms. *Front. Big Data* **4**, 613047. <https://doi.org/10.3389/fdata.2021.613047> (2021).
26. Yi, F. et al. XGBoost-SHAP-based interpretable diagnostic framework for alzheimer's disease. *BMC Med. Inf. Decis. Mak.* **23**. <https://doi.org/10.1186/s12911-023-02238-9> (2023).
27. Zou, M., Jiang, W. G., Qin, Q. H., Liu, Y. C. & Li, M. L. Optimized XGBoost model with small dataset for predicting relative density of Ti-6Al-4V parts manufactured by selective laser melting. *Mater. (Basel Switzerland)* **15**. <https://doi.org/10.3390/ma15155298> (2022).
28. Puttaert, D. et al. Decreased alpha peak frequency is linked to episodic memory impairment in pathological aging. *Front. Aging Neurosci.* **13**. <https://doi.org/10.3389/fnagi.2021.711375> (2021).
29. Tonner, P. H. & Bein, B. Classic electroencephalographic parameters: median frequency, spectral edge frequency etc. *Best Pract. Res. Clin. Anaesthesiol.* **20**, 147–159. <https://doi.org/10.1016/j.bpa.2005.08.008> (2006).
30. Goossens, J. et al. EEG dominant frequency peak differentiates between Alzheimer's disease and frontotemporal Lobar degeneration. *J. Alzheimer's Disease: JAD.* **55**, 53–58. <https://doi.org/10.3233/jad-160188> (2017).
31. Kwak, Y. T. & Quantitative EEG findings in different stages of Alzheimer's disease. *J. Clin. Neurophysiology: Official Publication Am. Electroencephalographic Soc.* **23**, 456–461. <https://doi.org/10.1097/01.wnp.0000223453.47663.63> (2006).
32. Foxe, J. J. & Snyder, A. C. The role of Alpha-Band brain oscillations as a sensory suppression mechanism during selective attention. *Front. Psychol.* **2**, 154. <https://doi.org/10.3389/fpsyg.2011.00154> (2011).
33. Bowman, A. D. et al. Relationship between alpha rhythm and the default mode network: an EEG-fMRI study. *J. Clin. Neurophysiol.* **34**, 527–533. <https://doi.org/10.1097/wnp.0000000000000411> (2017).
34. Babiloni, C. et al. Relationship between default mode network and resting-state electroencephalographic alpha rhythms in cognitively unimpaired seniors and patients with dementia due to Alzheimer's disease. *Cereb. Cortex* **33**, 10514–10527. <https://doi.org/10.1093/cercor/bhad300> (2023).
35. Law, Z. K. et al. The role of EEG in the diagnosis, prognosis and clinical correlations of dementia with lewy Bodies—A. *Syst. Rev. Diagnostics* **10**, 616 (2020).
36. Kantayeva, G., Lima, J. & Pereira, A. I. Application of machine learning in dementia diagnosis: A systematic literature review. *Heliyon* **9**, e21626. <https://doi.org/10.1016/j.heliyon.2023.e21626> (2023).
37. Torabinikjeh, M. et al. Correlations of frontal resting-state EEG markers with MMSE scores in patients with Alzheimer's disease. *Egypt. J. Neurol. Psychiatry Neurosurg.* **58**, 31. <https://doi.org/10.1186/s41983-022-00465-x> (2022).
38. Choi, J. et al. Resting-state prefrontal EEG biomarkers in correlation with MMSE scores in elderly individuals. *Sci. Rep.* **9**, 10468. <https://doi.org/10.1038/s41598-019-46789-2> (2019).
39. Park, Y. M. et al. Decreased EEG synchronization and its correlation with symptom severity in Alzheimer's disease. *Neurosci. Res.* **62**, 112–117. <https://doi.org/10.1016/j.neures.2008.06.009> (2008).
40. Ryu, H. J. & Yang, D. W. The Seoul neuropsychological screening battery (SNSB) for comprehensive neuropsychological assessment. *Dement. Neurocognitive Disorders* **22**, 1–15. <https://doi.org/10.12779/dnd.2023.22.1.1> (2023).
41. Huang, H. C., Tseng, Y. M., Chen, Y. C., Chen, P. Y. & Chiu, H. Y. Diagnostic accuracy of the clinical dementia rating scale for detecting mild cognitive impairment and dementia: A bivariate meta-analysis. *Int. J. Geriatr. Psychiatry.* **36**, 239–251. <https://doi.org/10.1002/gps.5436> (2021).
42. Brigham, E. O. & Morrow, R. E. The fast fourier transform. *IEEE Spectr.* **4**, 63–70. <https://doi.org/10.1109/MSPEC.1967.5217220> (1967).
43. Awad, M. & Fraihat, S. Recursive feature elimination with Cross-Validation with decision tree: feature selection method for machine Learning-Based intrusion detection systems. *J. Sens. Actuator Networks* **12**, 67 (2023).

Acknowledgements

We would like to thank Professor Sungkean Kim from Department of Human-Computer Interaction, Hanyang University, Ansan, Republic of Korea for his invaluable guidance and insightful feedback throughout the study.

Author contributions

K.I.J. and P.P. contributed to the conception and design of the study. S.J.A. contributed to the acquisition of data. K.I.J. and S.J.A. contributed to analysis of the data. K.I.J. and P.P. contributed to drafting the article. K.I.J., S.J.A., and P.P. contributed to the review of the article. K.I.J., S.J.A. and P.P. contributed to the supervision of the study. All authors approved the final version of the article.

Funding

This study was carried out with the support of R&D Program for Forest Science Technology (Project No. “FTIS 2021387D10-2323-0101”, and “2022438C10-2222-0102”) provided by Korea Forest Service (Korea Forestry Promotion Institute).

Declarations

Competing interests

The authors declare no competing interests.

Ethics declarations and informed consent statement

This study and all experimental protocols were approved by the International Review Board (IRB) of International St. Mary's Hospital (IRB Number: IS21OISE0035), Incheon, South Korea. Written informed consent was obtained from all participants. Our study conformed to the ethical guidelines of the World Medical Association Declaration of Helsinki.

Additional information

Correspondence and requests for materials should be addressed to S.J.A. or P.W.P.

Reprints and permissions information is available at www.nature.com/reprints.

Publisher's note Springer Nature remains neutral with regard to jurisdictional claims in published maps and institutional affiliations.

Open Access This article is licensed under a Creative Commons Attribution-NonCommercial-NoDerivatives 4.0 International License, which permits any non-commercial use, sharing, distribution and reproduction in any medium or format, as long as you give appropriate credit to the original author(s) and the source, provide a link to the Creative Commons licence, and indicate if you modified the licensed material. You do not have permission under this licence to share adapted material derived from this article or parts of it. The images or other third party material in this article are included in the article's Creative Commons licence, unless indicated otherwise in a credit line to the material. If material is not included in the article's Creative Commons licence and your intended use is not permitted by statutory regulation or exceeds the permitted use, you will need to obtain permission directly from the copyright holder. To view a copy of this licence, visit <http://creativecommons.org/licenses/by-nc-nd/4.0/>.

© The Author(s) 2025